ELSEVIER

Journal of Biomechanics 39 (2006) 2593–2602

JOURNAL OF BIOMECHANICS

www.elsevier.com/locate/jbiomech
www.JBiomech.com

The penetration of a soft solid by a liquid jet, with application to the administration of a needle-free injection

Oliver A. Shergold, Norman A. Fleck*, Toby S. King

Cambridge University Engineering Department, Trumpington St., Cambridge, CB2 1PZ, UK

Accepted 30 August 2005

Abstract

Liquid jet injections have been performed on human skin in vivo and silicone rubber using Intraject needle-free injectors. The discharge characteristics of the liquid jet were measured using a custom-built test instrument. The experiments reveal that a high-speed liquid jet penetrates a soft solid by the formation and opening of a planar crack. The fluid stagnation pressure required for skin penetration decreases with increasing diameter of the liquid jet. These findings are consistent with the slow-speed penetration of a soft solid by a sharp-tipped punch. It is demonstrated that the Shergold–Fleck sharp-tipped punch penetration model [Shergold, O.A., Fleck, N.A., 2004. Mechanisms of deep penetration of soft solids. Proc. Roy. Soc. Lond. A 460, 3037–3058.] gives adequate predictions for the pressure required to penetrate a soft solid by a high-speed liquid jet.

Keywords: Liquid jet injection; Fracture mechanics; Penetration; Skin; Rubber; Soft solid; Soft tissue

1. Introduction

The delivery of drugs by liquid injection is commonplace, with an estimated 12 billion skin injections given each year (Voelker, 1999). Typically, the delivery site is the dermal layer of the skin, or the underlying subcutaneous fat and muscle tissue. The conventional method of drug delivery is by injection using a needle and syringe. An alternative method of injection is to deliver the drug as a high-pressure liquid jet, of diameter in the range 0.1–0.5 mm, with sufficient intensity to pierce the skin. Commercially available needle-free syringes include the Intraject, J-Tip, Biojector 2000, Medi-ject Vision and Injex. A comparison of the main attributes of these needle-free devices is given in Table 1.

Liquid jet injection entails two sequential steps. The first step involves the penetration of the skin, fat and muscle tissue by a high-velocity liquid jet. In the second step, the bulk of the injectate is deposited within the target tissue at a lower velocity. This paper is concerned with the first step, and in particular the piercing of skin by a high-speed liquid jet.

The medical literature on skin injection and the mechanical engineering literature on rubber penetration each indicate that deep penetration by a sharp-tip solid penetrator involves cracking of the soft solid, followed by substantial reversible deformation after the penetrator has been removed (Stephens and Kramer, 1964; Katakura and Tsuji, 1985; Stevenson and Abmalek 1994; Shergold and Fleck, 2004a). A limited number of experimental studies reveal the sensitivity of crack geometry to the punch tip geometry and to the material properties of the penetrated solid (Stephens and Kramer, 1964; Katakura and Tsuji, 1985; Stevenson and Abmalek, 1994).

Shergold and Fleck (2004a) have demonstrated that a sharp-tipped punch penetrates human skin and silicone rubber by the formation of a planar mode I crack ahead of the tip, see Fig. 1a. The crack faces are wedged open by a punch that advances at a velocity v_P, see Fig. 1b.

*Corresponding author. Tel.: +44 1223 332650; fax: +44 1223 332622.
E-mail address: nafl@eng.cam.ac.uk (N.A. Fleck).

0021-9290/$ - see front matter © 2005 Elsevier Ltd. All rights reserved.
doi:10.1016/j.jbiomech.2005.08.028

Table 1
Comparison of currently available liquid injectors

Device	Intraject	J-Tip	Biojector 2000	Medi-Jector Vision	Injex
Parent company	Weston Medical (now Aradigm)	National Medical Products	Bioject	Antares Pharma	Equidyne Systems
Commercial launch	In development	1998	1993	1998	1999
Prefilled?	Yes	No	No	No	No
Single/multidose	Single	Single	Multi	Multi	Multi
Injection cartridge material	Glass	Plastic	Plastic	Plastic	Plastic
Length (mm)	120	110	220	—	140
Weight (g)	18	9	580	—	75
Price per unit ($)	1–2	1.5–2.0	600	~250	260
Price per syringe ($)	n/a	n/a	1.5	—	0.5–1.0
Energy Source	N_2 gas	CO_2 gas	CO_2 gas	Spring	Spring
Dose volume (ml)	0.5	0.02–0.5	<1.0	—	0.05–0.34
Operating temp. (°C)	2–40	10–37	14–38	10–29	5–30

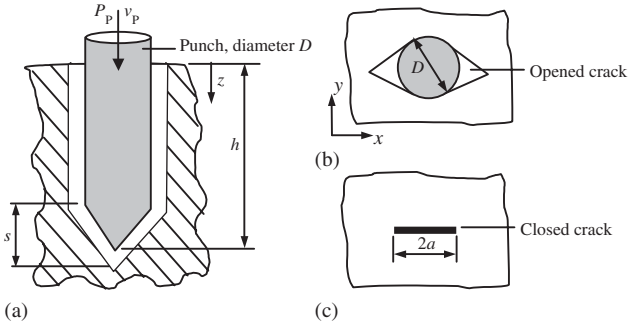

Fig. 1. (a) Penetration of a soft solid by a sharp-tipped punch, (b) crack opened to allow punch advance, (c) crack closed after punch removal.

Upon punch removal the planar crack closes (Fig. 1c), and in this undeformed configuration the crack has a length of $2a$. In this paper, we shall demonstrate experimentally that a high-speed liquid jet penetrates human skin and silicone rubber by the same mode I planar cracking mechanism as that observed for a sharp-tipped punch.

Shergold and Fleck (2004b) have proposed that the deep penetration of a soft solid by a sharp-tipped punch occurs by the mechanism shown in Fig. 1. The soft solid represents mammalian skin and silicone rubbers, and is treated as an incompressible, hyper-elastic, isotropic solid as described by a one-term Ogden (Ogden, 1972) strain energy density function of the form

$$\phi = \frac{2\mu}{\alpha^2}(\lambda_1^\alpha + \lambda_2^\alpha + \lambda_3^\alpha - 3), \quad (1)$$

where ϕ is the strain energy density per undeformed unit volume, α is a strain hardening exponent, μ is the shear modulus under infinitesimal straining and λ_i are the principal stretch ratios.

The Shergold–Fleck model predicts that the axial penetration pressure p_S on the shank of the punch increases with diminishing punch radius R, and with increasing mode I toughness J_{IC}, shear modulus μ and strain hardening exponent α. Here, we shall demonstrate that this deep penetration model can also be used to predict the threshold stagnation pressure of a high-speed liquid jet necessary to penetrate a soft solid such as silicone rubber or human skin.

Table 2 contains a review of the liquid jet characteristics taken from needle-free injector patents. In addition, a review of accidents involving high-pressure liquid jets (Vijay, 1989) and a review of needle-free injector designs (Maas and Brink, 1987) detail the combinations of liquid pressures and jet diameters that have penetrated human skin. These data are useful for indicating the *sufficient* condition for penetration, but give no insight into the threshold injection pressure for skin penetration, i.e., the *necessary* and *sufficient* condition. In broad terms, these data suggest that a pressure of 15 MPa is sufficient for the perforation of human skin by a liquid jet of diameter in the range 0.1–0.5 mm.

1.1. Outline of the paper

The structure of this paper is as follows. First, a set of experiments are described that identify the penetration mechanism for a high-speed liquid jet into human skin and silicone rubber, using the Intraject device (Weston Medical, now Aradigm). The stagnation pressure of the liquid jet required for penetration is measured. A prediction of the strain rate and crack growth rate associated with solid penetration is made, and the high strain rate mechanical properties (toughness and constitutive behaviour) of the penetrated solids are then determined from the literature. It is concluded that the sharp-tipped punch penetration model of Shergold and Fleck (2004b) are in broad agreement with the results of the liquid jet penetration experiments.

Table 2
Needle-free syringe patents that detail the discharge characteristics of the liquid jet

Publication date	Patent Number	Inventor	Company	Orifice diameter (mm)	Peak pressure (MPa)	Delivery pressure (MPa)
1943	US 2322245	Lockhart	—	0.1	71	—
1946	US 2398544	Lockhart	—	0.1	57–71	6.4
1955	US 2704543	Scherer	Scherer Corporation	0.08	71	14
1956	US 2754818	Scherer	Scherer Corporation	0.05–0.25	71	21
1956	US 2764977	Ferguson	Rutherford	0.08–0.25	—	12–15
1960	US 2928390	Venditty	Scherer Corporation	0.08–0.25	143	21
1974	US 3853125	Clark and Hollenbeck	—	0.2	—	8–12
1977	US 4059107	Iriguchi et al.	Asahi	0.1–0.2	12	10
1988	US 4790824	Morrow and Burns	Bioject	0.2	36–43	—
1988	US 4722728	Dixson	—	0.1–0.2	>70	20
1989	US 4874367	Edwards	Marpam Intl	0.125	5.7	—
1994	US 5312335	McKinnon et al.	Bioject	0.1–0.6	21–43	—
1995	WO 95/25555	Salo et al.	Vitajet Corporation	0.15	18–32	—
1995	US 5399163	Peterson et al.	Bioject	0.08–0.13	28–31	8–14
1996	US 5520639	Peterson et al.	Bioject	0.1–0.15	29	9–14
1997	US 5599302	Lilley et al.	Medi-Ject	0.17	—	—
1998	WO 98/31409	Haar et al.	Boehringer Mannheim	0.08–0.10	30–60	10–60
1998	US 5730723	Castellano and Schumecher	Visionary Medical Products	0.08	30–67	—
2001	WO 01/13977	Stout et al.	Bioject	0.1	28	23
2001	WO 01/13977 A1	Stout et al.	Bioject	0.1	28–31	20–27
2001	EP 1 125 593 A1	Haar	Roche	0.2	30	20
2001	WO 01/47586 A1	Neracher	—	0.05	200	100
2002 Application	US 2002/0058907 A1	Deboer et al.	Medi-Ject	0.1–0.34	29	—
	EP 0 651 663 B1	Peterson and McKinnon	Bioject	0.1	27–30	8.2–14

2. Experiments

Injection experiments were performed on both human skin and B452 silicone rubber using a set of Intraject devices to identify the mechanisms of perforation. Full details on the B452 silicone rubber are given in the companion paper of Shergold and Fleck (2004a); this previous paper focuses on the deep penetration of silicone rubbers by solid cylindrical punches. In the current study on liquid jets, the threshold value of stagnation pressure is measured for the successful penetration of human skin and B452 silicone rubber; and the sensitivity of this penetration pressure to the diameter of liquid jet is explored. Informed consent was given by all of the subjects participating in the skin penetration experiments.

2.1. Description of the intraject liquid jet injector

The Intraject device shown in Fig. 2 was used for the liquid jet injection trials. The device is operated as follows. A sterile drug container is sealed at one end by a piston, and has an orifice at the other end through which the drug is ejected. A stopper held within a plastic sleeve seals the orifice and maintains drug sterility. Immediately prior to injection the plastic sleeve and stopper are removed to expose the orifice, and the orifice is placed in contact with the surface of the skin. On triggering the device a steel ram is accelerated by pressured nitrogen gas. The ram impacts the piston and thereby generates a high-pressure pulse in the drug. This high-pressure pulse causes 1–10% of the drug dose to be ejected at high velocity (on the order of $200\,m\,s^{-1}$) from the container, and this initial liquid jet perforates the skin. Subsequently, the pressure in the remaining drug within the device drops to a lower level; most of the dose (90–99%) is then ejected through the orifice at the lower liquid pressure and lower velocity (on the order of $150\,m\,s^{-1}$), and is delivered through the perforated dermis.

A set of Intraject devices were customised to provide a range of values of peak pressure and delivery pressure. To achieve this, the gas cylinder pressure was varied, and the impact gap between the ram and the piston was adjusted by a combination of moving the piston and

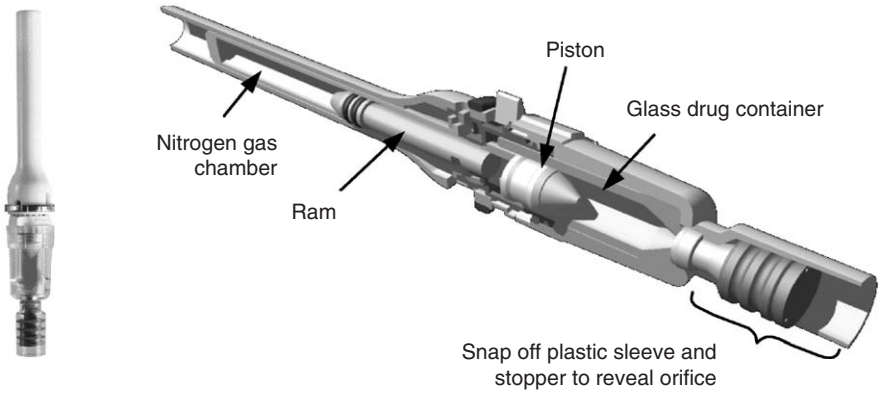

Fig. 2. Intraject used for liquid injection experiments: (a) in side profile, and (b) in cross-section.

changing the length of the ram. An increase in the impact gap increases the peak pressure of the liquid jet without altering the subsequent delivery pressure, whilst an increase in the gas cylinder pressure leads to an increase in both the peak pressure and the delivery pressure.

The diameter of the orifice in the drug capsule was varied within the range 0.25–0.50 mm in order to control the diameter of the liquid jet. Note that the diameter of the orifice is an order of magnitude smaller than the bore of the drug container; consequently, any variation in the orifice diameter has a negligible effect upon the stagnation pressure versus time response in the early stages of injection. The duration of the injection is dictated by the diameter of the orifice.

2.2. Measurement of the liquid jet stagnation pressure versus time response

The discharge characteristic of each Intraject configuration used in the penetration experiments was measured using a Jet Tester. The Jet Tester was also used to measure the jet characteristics of the J-Tip, Biojector, 2000, Medi-ject Vision and Injex devices.

A sketch of the Jet Tester is given in Fig. 3. The liquid jet injector is clamped vertically above a steel target. In turn, the target is connected to a force transducer (Kistler, 9207), and thereby to a charge amplifier (Kistler 5011B10). When the device is fired, the liquid jet impinges the target, and generates a force by the change in momentum flux. This force is recorded by a PC-based data acquisition system.

The liquid jet velocity versus time response is calculated from the recorded force versus time response as follows. Fig. 4 shows the liquid jet as it impinges the Jet Tester target. Prior to impingement, the jet has a velocity v_z normal to the target and a cross-sectional area of A. After impact the liquid flows parallel to the target surface and $v_z = 0$. The momentum flux of the liquid jet perpendicular to the target surface is given by

$$F = \rho A v_z^2, \tag{2}$$

where F is the measured reaction force of the jet impact upon the target, and ρ is the density of the liquid.

The volume of fluid V ejected during the test is given by

$$V = \int_0^t A v_z \, \mathrm{d}t. \tag{3}$$

Assume that V is measured. Then the cross-sectional area of the jet is calculated by combining Eqs. (2) and (3) to obtain

$$A = \rho \left[\frac{V}{\int_0^t \sqrt{F} \, \mathrm{d}t} \right]^2 \tag{4}$$

and the instantaneous velocity v_z follows immediately as

$$v_z = \sqrt{\frac{F}{\rho A}}. \tag{5}$$

Bernoulli's equation is then used to infer the stagnation pressure versus time response of the liquid inside the drug container from the velocity versus time response of the liquid jet. This calculation assumes that the nozzle is loss-free.

The stagnation pressure measured by the Jet Tester has been validated by mounting strain gauges onto the outside wall of an Intraject glass capsule and calculating the liquid pressure inside the capsule from the measured hoop strain.

2.3. Human skin penetration experiments

2.3.1. Study to determine the penetration mechanism of human skin

About 0.5 ml of saline was injected into the abdomen of five volunteers using Intraject devices with an orifice of diameter 0.34 mm, a gas cylinder pressure of 23 MPa and an

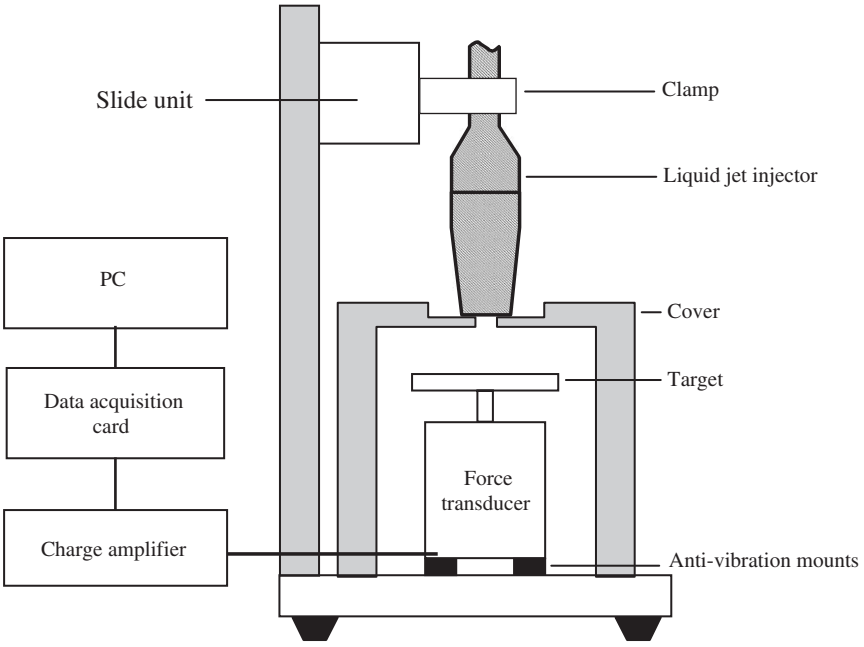

Fig. 3. Sketch of the Jet Tester used to measure the discharge characteristics of a liquid jet issuing from a needle-free syringe.

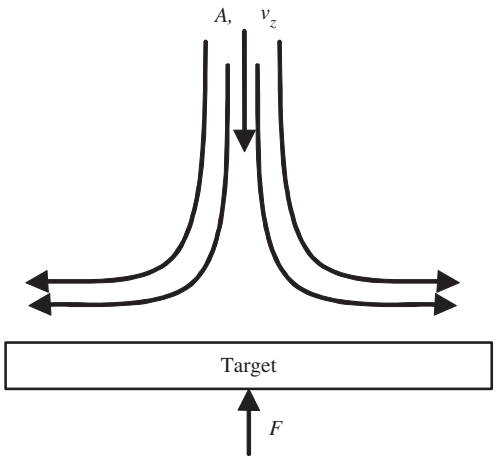

Fig. 4. Sketch of the liquid jet as it leaves the injector orifice and impacts upon the target of the Jet Tester.

impact gap of 3 mm. Images of the injection sites were taken by lightly pushing the skin against a disposable, transparent, plastic end cap fitted onto the end of a stereoscopic microscope. The end cap set the required focal distance and prevented relative movement between the camera and the abdomen. Images were taken within seconds of the injection and 1.5 h later. Clear images of the injection site immediately after injection were difficult to achieve due to slight seepage of blood from the injection site.

2.3.2. Study to determine the minimum pressure to inject human skin

A series of Intraject injections were performed on two volunteers in order to determine the minimum pressure for skin penetration. The procedure was as follows. Intraject devices were manufactured with an orifice of diameter 0.34 mm, and the gas cylinder pressures was set at the selected values of 10, 16, 23 and 27 MPa. A brass disc, of diameter 6.8 mm and thickness 3.8 mm, was placed between the piston and the ram in order to eliminate the impact gap (yet maintain the piston away from the non-sterile, open end of the drug container).

Injections were administered into the abdomen of the two volunteers, starting with the lowest gas pressure. The injection site was examined after the device had been fired to determine if the liquid jet had perforated the outer surface of the skin. Skin penetration was identified by a distinctive red mark and the ability to squeeze out a small drop of blood. Photographs were taken of the injection site with a hand-held digital camera.

2.4. B452 silicone rubber penetration experiments

A series of Intraject devices were manufactured in order to investigate the minimum pressure required to penetrate a B452 rubber block. The devices had an orifice of diameter 0.34 or 0.50 mm, and a gas cylinder pressure of 23 MPa. The peak stagnation pressure was varied by adjusting the impact gap between 0 and 5 mm. Devices were fired into blocks of the B452 rubber and the front surface was examined for signs of penetration. Finally, the block was sectioned diametrically to reveal the depth of liquid jet penetration.

3. Results

3.1. Liquid jet discharge characteristics

Jet Tester measurements of the stagnation pressure versus time response of the liquid jet ejected from an Intraject, J-Tip, Biojector 2000, Medi-ject Vision and Injex are shown in Fig. 5. The characteristics of each device, and the calculated ratio of the calculated jet area to measured orifice area A/A_0, are given in Table 3.

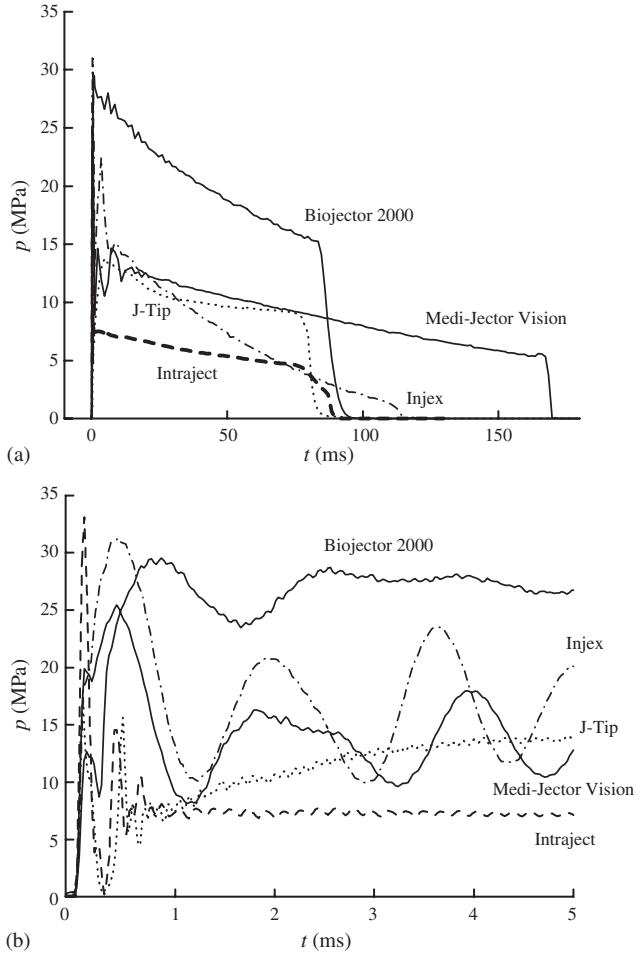

Fig. 5. (a) Stagnation pressure versus time response of a liquid jet discharging from a needle-free injector measured using the Jet Tester, (b) detail of the first 5 ms of the stagnation pressure versus time response.

All of these needle-free syringes have similar discharge characteristics: there is a high-pressure pulse during the first 1–5 ms of the injection, followed by a steady decay in liquid pressure over the remaining 80–160 ms. The peak liquid stagnation pressure arises from the impact of the ram against the piston at the start of the injection. Of all the devices tested, the Intraject device has the largest ratio of peak pressure (35 MPa) to average delivery pressure (6 MPa).

3.2. Pressure required to penetrate human skin and B452 rubber

The initial, peak value of stagnation pressure sufficient for the deep penetration of human skin and B452 silicone rubber is given in Table 4. The measured penetration pressure of 14 MPa for human skin by a liquid jet of diameter 0.34 mm is consistent with the value of 15 MPa sufficient for penetration as highlighted by our review on liquid jet injector patents. Table 4 includes the peak liquid jet stagnation pressure that indented but did not penetrate each solid. Hence, the minimum value of liquid stagnation pressure required to penetrate each solid lies between these two limits.

The experiments demonstrate that the penetration pressure of B452 rubber is greater than that of human skin, and the penetration pressure increases with a diminishing diameter of liquid jet. These findings are similar to the sharp-tipped punch penetration experiments of Shergold and Fleck (2005a). A comparison of the investigations reveals that a liquid jet requires double the pressure to penetrate human skin or B452 rubber compared with a sharp-tipped punch of equal diameter.

3.3. Penetration mechanism of a soft solid by a high-speed liquid jet

Photographs of the injection site show that a liquid jet penetrates a soft solid by the formation of planar crack that opens to accommodate fluid flow. This penetration mechanism is similar to that of a soft solid by a sharp-tipped punch (Shergold and Fleck, 2005a), as shown in Fig. 1. Examples of cracking on the surface of human skin and B452 silicone rubber are given in Fig. 6. Sections taken perpendicular to the front face of the

Table 3
Measured and calculated liquid jet characteristics for different needle-free injectors

	Intraject	Bioject	Medi-Jector	J-Tip	Injex
Delivered dose (ml)	0.5	0.5	0.5	0.25	0.25
Orifice diameter (μm)	300	110	200	210	165
Jet diameter (μm)	308	124	168	163	157
A/A_0	1.05	1.27	0.71	0.60	0.91

Table 4
Peak stagnation pressure of a liquid jet that leads to either indentation or penetration of human skin or B452 silicone rubber

Solid	Human skin	B452 silicone rubber	
Liquid jet diameter (mm)	0.34	0.34	0.500
Indentation pressure (MPa)	10	30	14
Penetration pressure (MPa)	14	34	21

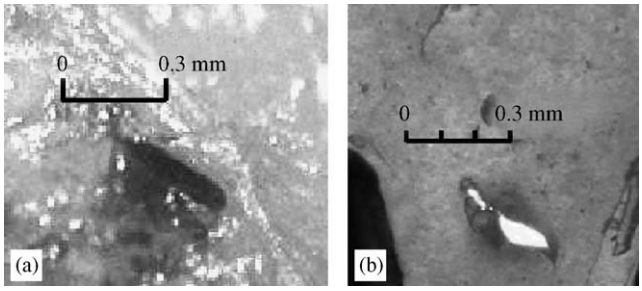

Fig. 6. Penetration of (a) human skin, and (b) B452 silicone rubber by a ∅0.34 mm high-speed liquid jet results in a planar crack.

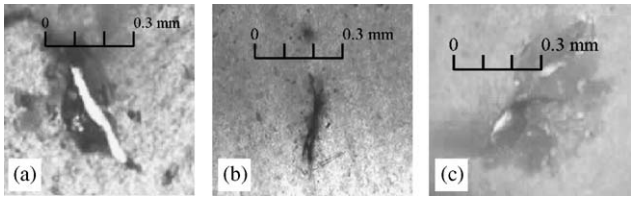

Fig. 7. Cracking at (a) 0.1 mm, (b) 0.9 mm and (c) 1.3 mm depth into a B452 rubber block following penetration by a ∅0.34 mm orifice, 3 mm impact gap Intraject with a gas pressure of 23 MPa.

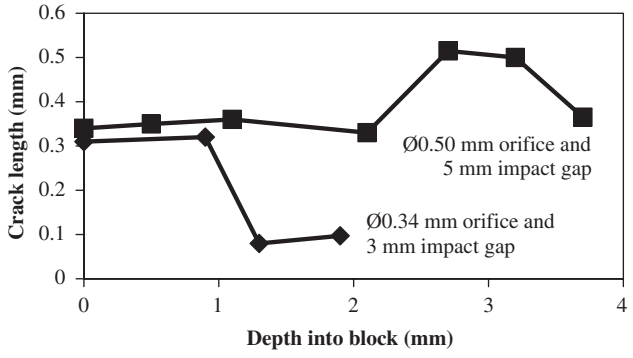

Fig. 8. Crack length versus depth into block of B452 rubber following injection with a ∅0.34 mm orifice Intraject with a 3 mm impact gap and a ∅0.50 mm orifice Intraject with a 5 mm impact gap.

B452 rubber block a posteriori demonstrate that the crack extends deep into the block. Fig. 7 shows the crack geometry at depth into the B452 rubber block.

Fig. 8 shows the length of the crack at different depths into the B452 rubber block following penetration by a liquid jet of diameter 0.34 and 0.50 mm. In the case of the liquid jet of diameter 0.34 mm, the crack length is almost constant within increasing penetration. In contrast, for the liquid jet of diameter 0.50 mm, the crack lengthens at depth. Two possibilities exist for this crack lengthening, as follows.

One explanation is provided by the sharp-tipped punch penetration experiments of Shergold and Fleck (2005a), which showed that the crack length was smaller at the surface than at depth. It is found that a higher punch load and a greater deformation of the solid is required for crack initiation compared with crack propagation.

An alternative explanation for the shorter crack length near the surface of the block may be that the velocity of the crack is limited by the elastic shear wave speed of the soft solid. In the following section, we estimate that the crack velocity associated with the penetration of B452 silicone rubber or human skin is on the order of $30\,\mathrm{m\,s^{-1}}$. This speed is comparable to the typical shear wave speed of rubber (about $50\,\mathrm{m\,s^{-1}}$) (Lake et al., 2000). The inertial limitation of crack speed during penetration of the B452 rubber block may explain why the crack length during the first 2 mm of penetration is similar for the liquid jets of diameter 0.34 and 0.50 mm.

4. A comparison of the experiments with the sharp-tipped punch penetration model

The sharp-tipped punch penetration model of Shergold and Fleck (2004) reveals that the dimensionless penetration pressure p_S/μ across the shank of the punch increases with the dimensionless group $J_{IC}/\mu R$ and with increasing strain hardening exponent α. In order to compare the predictions of the model with experimental results, values for the mechanical properties of human skin and B452 rubber are determined from the literature. However, to determine the appropriate mechanical properties, consideration must be given to the solid strain rate and crack growth rate during liquid jet penetration.

A representative strain rate is given by $\dot{\varepsilon} \approx \dot{a}/a$ where $2a$ is the final crack length as developed by the liquid jet, and $\dot{a}$ is the average crack velocity. The crack length a is on the order of 0.3 mm, see Fig. 8, and the event time for

the liquid jet to establish the crack length is estimated to be 100 μs: this is the width of the initial pressure spike for the Intraject device, as shown in Fig. 5b. Consequently, we assume a crack speed of $30\,\mathrm{m\,s^{-1}}$ and a representative strain rate of $1\times10^4\,\mathrm{s^{-1}}$.

4.1. Mechanical properties of silicone rubber and skin

4.1.1. Constitutive response

Shergold and Fleck (2005b) measured the uniaxial compressive stress versus strain response of B452 silicone rubber and pig skin across a wide range of nominal strain rates (0.004–$4000\,\mathrm{s^{-1}}$) and found Ogden fits to each measured response. They demonstrated that the strain rate sensitivity of silicone rubber and pig skin can be adequately described by an increase in the shear modulus μ of the solid with increasing strain rate, whilst the strain hardening exponent α remains constant.

In order to make predictions for the penetration resistance of B452 silicone rubber at a representative strain rate of $1\times10^4\,\mathrm{s^{-1}}$, we shall make use of the measured value of $\mu=17\,\mathrm{Mpa}$. Unfortunately, no high strain rate data on human skin could be gleaned from the literature, and so the high-strain response was estimated from the low-strain rate measurements by Jansen and Rottier (1958), and then scaled to account for the effect of strain rate. (The same scale factor was used as that measured for pig skin by Shergold and Fleck (2005b).) Jansen and Rottier (1958) measured the tensile stress versus strain response of human skin samples taken 80 mm laterally from the median line between the umbilic and pubic area at a strain rate of $0.01\,\mathrm{s^{-1}}$. Shergold and Fleck (2005a) found a reasonable fit to Jansen and Rottier's data using a one-term Ogden function ($\mu=0.11\,\mathrm{MPa}$, $\alpha=9$). The high strain rate response of human skin was thereby estimated to be ($\mu=1.7\,\mathrm{MPa}$, $\alpha=9$).

4.1.2. Toughness

Only limited data exist on the toughness of skin and silicone rubber as a function of crack velocity. Consequently, only approximate estimates can be made for the mode I toughness of skin and B452 rubber at crack growth rates on the order of $30\,\mathrm{m\,s^{-1}}$. Pereira et al. (1997) measured the toughness of human skin ($J_C=2.5\,\mathrm{kJ\,m^{-2}}$) at a crack growth rate of $0.4\,\mathrm{mm\,s^{-1}}$ using a scissor tear test, whereas Shergold (2004) used a trouser tear test to determine the toughness ($J_C=3.8\,\mathrm{kJ\,m^{-2}}$) of B452 rubber at a crack growth rate of $0.2\,\mathrm{m\,s^{-1}}$.

Mixed mode crack propagation studies on mammalian tissue (Purslow, 1983a b; Pereira et al., 1997) and rubber (De and Gent, 1996; Greensmith and Thomas, 1955; Lake and Yeoh, 1978; Lake and Yeoh, 1987) suggest that the measured toughness J_{IC} is sensitive to the type of test performed. Scissor cutting tests and razor cutting tests maintain a sharp crack tip and give a low-toughness value. In contrast, the trouser tear test allows the crack tip to blunt and thereby gives rise to a larger measured toughness. This is consistent with the fact that the toughness of rat skin as measured by a trouser tear test (Purslow, 1983a) is an order of magnitude higher than that measured by a scissor tear test (Pereira et al., 1997).

It is not obvious whether a trouser tear test or scissor tear test provides the most representative toughness value for the penetration of a soft solid by a liquid jet. Here, we assume $J_{IC}=2.5\,\mathrm{kJ\,m^{-2}}$ for human skin and $3.8\,\mathrm{kJ\,m^{-2}}$ for the B452 rubber.

4.2. Comparison of the penetration model and experimental results

The prediction of the sharp-tipped punch penetration model (Shergold and Fleck 2004) for the relationship between p_S/μ and $J_{IC}/\mu R$ and α is shown in Fig. 9a for solids with $\alpha=3$, representative of the B452 rubber, and

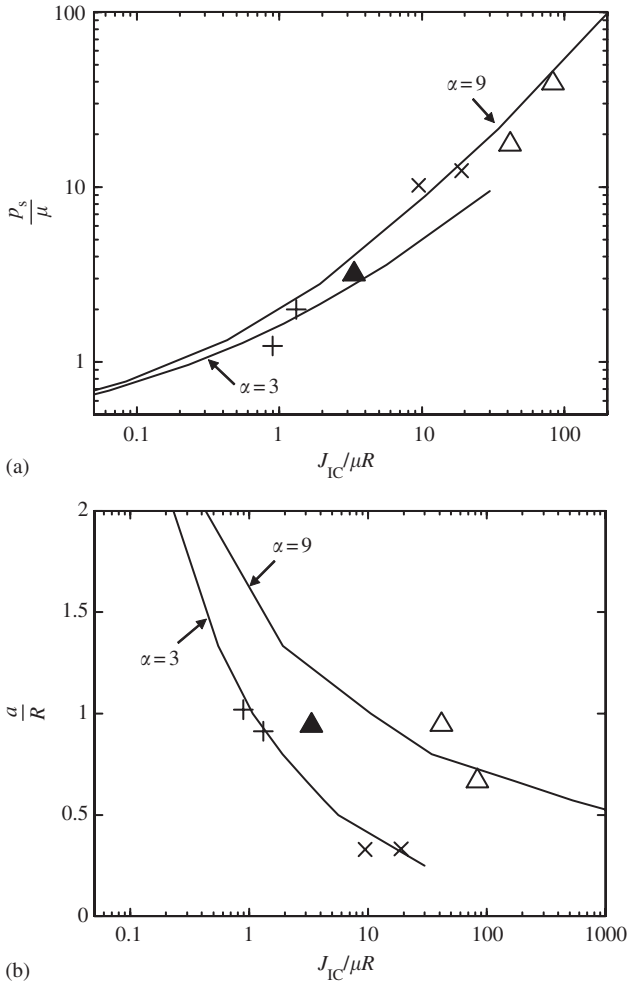

Fig. 9. (a) p_S/μ versus J_{IC}/μR and (b) a/R versus J_{IC}/μR, for penetration of a soft solid by a sharp punch and a liquid jet.

for human skin with $\alpha = 9$. The predicted dimensionless crack length a/R resulting from punch penetration is shown in Fig. 9b. The measured values of p_S/μ and a/R from the liquid jet injection experiments are included in Fig. 9 using the value of $J_{IC}/\mu R$ that gave the best agreement with the predicted values ($J_{IC} = 3.8\,kJ\,m^{-2}$ for the B452 rubber and for human skin, $J_{IC} = 2.5\,kJ\,m^{-2}$). The measured orifice radius of the capsule is used as the value for R. The sharp-tipped punch penetration experiments of Shergold and Fleck (Shergold and Fleck 2005a) are included in Fig. 9. Shergold and Fleck used a $\varnothing 1.0$ mm and $\varnothing 2.0$ mm conical-tipped punch to penetrate B452 rubber at a punch velocity of $0.8\,mm\,s^{-1}$, and a $\varnothing 0.3$ mm and $\varnothing 0.6$ mm hypodermic needle to penetrate human skin at a punch velocity of $1\,mm\,s^{-1}$. Reasonable agreement exists between the model predictions and the measurements, but the level of agreement is sensitive to the assumed values of mechanical properties. Further work is required to measure modulus over a wide range of strain rates and toughness over a wide range of crack speeds.

The sharp-tipped punch penetration model can be compared with the reported values of skin penetration pressure for the various liquid jet injector designs. In Fig. 10, the predicted pressure required to penetrate human skin is plotted against the liquid jet diameter for skin mechanical properties of $J_{IC} = 2.5\,kJ\,m^{-2}$, $\mu = 1.7$ MPa and $\alpha = 9$. The peak stagnation pressure and liquid jet diameter of each needle-free syringe measured by the Jet Tester are included, as well as the needle-free syringes as described in the patents listed in Table 2.

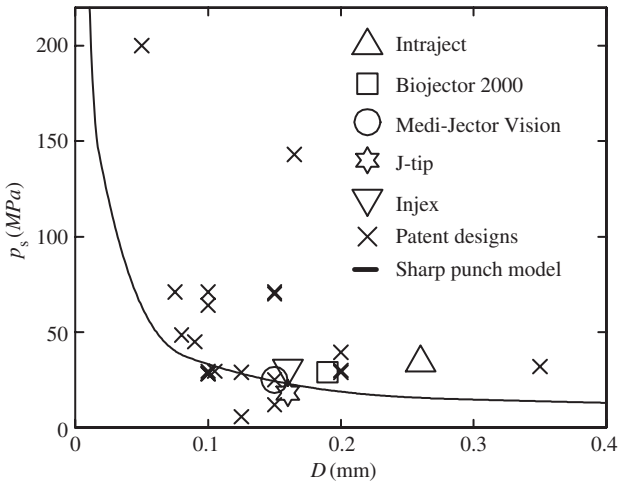

Fig. 10. Sharp-tipped punch model prediction for the relation between the liquid stagnation pressure p_S and the liquid jet diameter D for penetration of human skin, ($J_{IC} = 2.5\,kJ\,m^{-2}$, $\mu = 1.7$ MPa, $\alpha = 9$). Also shown is the peak stagnation pressure versus jet diameter of various needle-free syringes.

The general trend is for the peak stagnation pressure for successful injection by the needle-free syringes to increase with diminishing jet diameter. There is reasonable agreement between the model and the operating pressure of the needle-free syringes. The majority of injector designs lie close to the predicted penetration pressure, and these designs would be expected to penetrate the skin, for example the Biojector 2000 or Intraject devices. Devices that lie significantly below the predicted curve will be less likely to inject human skin.

5. Concluding remarks

Liquid jet injection into human skin in vivo and into B452 silicone rubber blocks demonstrate that the penetration of a soft solid is by the formation and opening of a planar crack. This penetration mechanism is similar to that observed in the penetration of a soft solid by a sharp-tipped punch. A liquid jet of diameter 0.34 mm requires a stagnation pressure of approximately 14 MPa to penetrate human skin, and approximately 34 MPa to penetrate B452 silicone rubber. These penetration pressures are twice that required for a sharp-tipped punch of equal diameter.

The Intraject needle-free syringe has a high stagnation pressure (35 MPa) at the start of the injection followed by a low stagnation pressure (6 MPa) during the delivery of the bulk of the injectate. For this device skin penetration occurs only during the initial stages of the injection, enabling the depth of penetration to be controlled.

A penetration model proposed for the deep penetration of a soft solid by a sharp-tipped punch provides a reasonable prediction for the penetration pressure of a high-speed liquid jet. The predicted penetration pressure is sensitive to the shear modulus and mode I toughness of the solid.

Acknowledgements

The authors are grateful for funding from Weston Medical, the Engineering and Physical Sciences Research Council and the Royal Commission for the Exhibition of 1851.

References

De, D., Gent, A.N., 1996. Tear strength of carbon-black-filled compounds. Rubber Chemistry and Technology 69 (5), 834–850.

Greensmith, H.W., Thomas, A.G., 1955. Rupture of rubber III. Determination of tear properties. Journal of Polymer Science 18, 189–200.

Jansen, L.H., Rottier, P.B., 1958. Some mechanical properties of human abdominal skin measured on excised strips: a study of their

dependence on age and how they are influenced by the presence of striae. Dermatologica 117, 65–183.

Katakura, H., Tsuji, S., 1985. A study to avoid the dangers of high-speed liquid jets. Bulletin of JSME 28 (238), 623–630.

Lake, G.J., Lawrence, C.C., et al., 2000. High-speed fracture of elastomers: Part I. Rubber Chemistry and Technology 73, 801–817.

Lake, G.J., Yeoh, O.H., 1978. Measurement of rubber cutting Resistance in the absence of friction. International Journal of Fracture 14 (5), 509–526.

Lake, G.J., Yeoh, O.H., 1987. Effect of crack tip sharpness on the strength of vulcanized rubbers. Journal of Polymer Science Part B: Polymer Physics 25 (6), 1157–1190.

Maas, A.J., Brink, P.R.G., 1987. Some physical aspects of the medical jet injector. Medical and Biological Engineering and Computing 25, 81–86.

Ogden, R.W., 1972. Large deformation isotropic elasticity—on the correlation of theory and experiment for incompressible rubberlike solids. Proceedings of the Royal Society of London A 326, 565–584.

Pereira, B.P., Lucas, P.W., et al., 1997. Ranking the fracture toughness of thin mammalian soft tissues using the scissors cutting test. Journal of Biomechanics 30 (1), 91–94.

Purslow, P., 1983a. Measurement of the fracture toughness of extensible connective tissues. Journal of Materials Science 18, 3591–3598.

Purslow, P.P., 1983b. Positional variations in fracture toughness, stiffness and strength of descending thoracic pig aorta. Journal of Biomechanics 18 (11), 947–953.

Shergold, O., 2004. The Mechanics of Needle-free Injection. Department of Mechanical Engineering, Cambridge University, Cambridge, p. 200.

Shergold, O., Fleck, N. A., 2004. Mechanisms of deep penetration of soft solids, with application to the injection and wounding of skin. Proceedings of the Royal Society, London, Series A 460, 3037–3058.

Shergold, O., Fleck, N. A., 2005a. Experimental investigation into the deep penetration of soft solids by sharp and blunt punches, with application to the piercing of skin. Journal of Biomechanical Engineering 127, 838–848.

Shergold, O., Fleck, N. A., 2005b. The uniaxial constitutive behaviour of pig skin and silicone rubber across a wide range of strain rates. International Journal of Impact Engineering, to appear.

Stephens, R.R., Kramer, I.R.H., 1964. Intra-oral injections by high-pressure jet. British Dental Journal 117 (11), 465–476.

Stevenson, A., Abmalek, K., 1994. On the puncture mechanics of rubber. Rubber Chemistry and Technology 67 (5), 743–760.

Vijay, M. M., 1989. A critical examination of the use of water jets for medical applications. In: Fifth American Water Jet Conference, Toronto, Canada, National Research Council of Canada.

Voelker, R., 1999. Eradication efforts need needle-free delivery. JAMA 281 (20), 1879–1881.